Metabolomics as an Extension of Proteomic Analysis: Study of Acute Kidney Injury

Didier Portilla, MD, Laura Schnackenberg, PhD,† and Richard D. Beger, PhD†*

Summary: Although proteomics studies the global expression of proteins, metabolomics characterizes and quantifies their end products: the metabolites, produced by an organism under a certain set of conditions. From this perspective it is apparent that proteomics and metabolomics are complementary and when joined allow a fuller appreciation of an organism's phenotype. Our studies using ^{1}H-nuclear magnetic resonance spectroscopic analysis showed the presence of glucose, amino acids, and trichloroacetic acid cycle metabolites in the urine after 48 hours of cisplatin administration. These metabolic alterations precede changes in serum creatinine. Biochemical studies confirmed the presence of glucosuria, but also showed the accumulation of nonesterified fatty acids, and triglycerides in serum, urine, and kidney tissue, despite increased levels of plasma insulin. These metabolic alterations were ameliorated by the use of fibrates. We propose that the injury-induced metabolic profile may be used as a biomarker of cisplatin-induced nephrotoxicity. These studies serve to illustrate that metabolomic studies add insight into pathophysiology not provided by proteomic analysis alone.

Semin Nephrol 27:609-620

Keywords: *Metabolomics, acute kidney injury, cisplatin, nuclear magnetic resonance, mass spectrometry*

Transcriptomics, proteomics, and metabolomics technologies comprise what is referred to as *systems biology*. The hope is that these "omics" technologies will identify translational biomarkers that are applicable to both preclinical investigations and in the clinical setting. This is especially true for markers of acute kidney injury, in which traditional serum markers such as blood urea nitrogen and creatinine have proven to be insensitive and nonspecific.[1] ***Metabolomics*** refers to the study of metabolite pool that exists within a cell, tissue, or biofluid under a particular set of conditions,[2] whereas *metabonomics* has been defined as the "quantitative measurement of the dynamic metabolic response of living systems to pathophysiological stimuli or genetic modification."[3] Metabolomics, metabonomics, or global metabolic profiling use analytic technologies such as nuclear magnetic resonance (NMR) spectroscopy and mass spectrometry (MS) to identify and quantify as many metabolites as possible in cells, tissues, and biofluids. The quantified metabolites then can be evaluated statistically to determine biomarkers of health and disease status and to help elucidate mechanisms of drug metabolism and drug toxicity.

Typically, changes in metabolite levels represent the downstream changes in the genome and the proteome, but in reality they represent not only changes in gene function but also are influenced by factors related to environment and phenotype.[2] Further, up-regulation or down-

*Department of Nephrology, University of Arkansas for Medical Sciences, Little Rock, AK.

†Division of Systems Toxicology, National Center for Toxicological Research, Jefferson, AR.

Supported by a VA Merit Award Grant and National Institutes of Health/ National Institute for Diabetes and Digestive Kidney Diseases (RO1-DK075976 to D.P.).

The views presented in this article do not necessarily reflect those of the US Food and Drug Administration.

Address reprint requests to Dr. Didier Portilla, Department of Nephrology, University of Arkansas for Medical Sciences, 4301 W. Markham St, Little Rock, AK 72205. E-mail: dportilla1@uams.edu

0270-9295/07/$ - see front matter

 doi:10.1016/j.semnephrol.2007.09.006

regulation of a particular transcript does not necessarily result in an instantaneous change in enzymatic activity.[4] This means that it is important to investigate the changes in gene transcripts, proteins, and metabolites over multiple time points to understand their interactions at a systems level. In this case, metabolic profiling studies have the advantage in terms of ease of sample collection of biofluids, preparation, and analysis. Therefore, metabolic profiling–derived data can be used to pinpoint time points of interest for further genomics and proteomics studies.

Metabolic profiling studies will be critical in forwarding the concept of personalized medicine because the metabolic profile encodes information about both the phenotype and the genotype.[2] Phenotype is influenced by numerous environmental factors including health to disease status, gut microflora content, nutritional intake, and age, among others. The bottleneck of metabolic profiling is trying to understand the link between metabolites and their phenotype or genotype information, which requires a strong bioinformatics component and the proper experimental design. This being said, an individual's metabolic profile, therefore, reflects both genotype and phenotype information, which can be used by health care providers to provide more accurate health to disease assessment and individualized medical treatment. NMR has been used to study renal toxicity,[5-10] hepatotoxicity,[5,10-13] renal transplants,[14] cancer,[15,16] and atherosclerosis.[17,18] NMR is used widely because it is relatively simple to use for high-throughput analyses of biofluids such as urine or serum.

METABOLOMIC STUDY OF CISPLATIN-INDUCED ACUTE RENAL FAILURE

Nephrotoxicity is a common side effect of cisplatin-based chemotherapeutic regimens.[19-22] Our previous studies showed reduced protein expression and enzyme activities of several kidney peroxisome proliferator-activated receptor α (PPARα) target genes in response to cisplatin nephrotoxicity, and also that the use of PPARα ligands such as fibrate compound WY-14,643 protected renal function by preventing proximal tubule cell death in the animal models of ischemia-reperfusion and cisplatin-induced acute renal failure (ARF). We have examined the metabolic alterations that occur in ARF using high-resolution ^{1}H NMR spectroscopy coupled with pattern recognition.[9] Experimental ARF was induced in 8- to 10-week-old male mice (strain Sv129) using cisplatin administration. Animals were maintained on standard chow and, as indicated, a group of animals was fed with a special diet containing fibrate compound WY-14,643 (1% wt/wt) for 7 days before the induction of ARF. Cisplatin was administered by a single intraperitoneal injection of 20 mg cisplatin/kg/body weight. After the induction of renal failure, the animals were returned to their cages and allowed free access to food and water. Urine samples were collected for NMR analysis and biochemical measurements of metabolite concentration at days 1, 2, and 3 after cisplatin administration. Urine samples were analyzed on a Bruker Avance NMR spectrometer (Billerica, MA) equipped with a triple-resonance cryoprobe. A standard water-suppression pulse program was used for the presaturation of the water peak. In the studies in which the PPARα ligand WY compound was used, urine samples obtained after 2 days of cisplatin injection were analyzed because the urine metabolic profile at this point was quite different from the one obtained from control mice. Spectra were Fourier-transformed, phased, baseline corrected, and intelligently binned using ACD/Labs 1D NMR Manager, version 9.0 (ACD/Labs, Toronto, Canada). Individual spectra were exported as jcamp files for further analysis by Chenomx Eclipse software (Chenomx, Edmonton, Canada). Chenomx Eclipse software and databases were applied for identification of specific metabolites in the spectra.

Metabolic Changes in Urine Samples by ^{1}H-NMR

Figure 1 shows representative spectra from the urine of the same mouse obtained before dosing, and for 3 days after dosing with 20 mg cisplatin/kg/body weight. Visual inspection of the spectra showed changes in various urine metabolites after the mouse had been given a dose of cisplatin, including increases in glucose, lactate, pyruvate, and 2-oxoglutarate 48

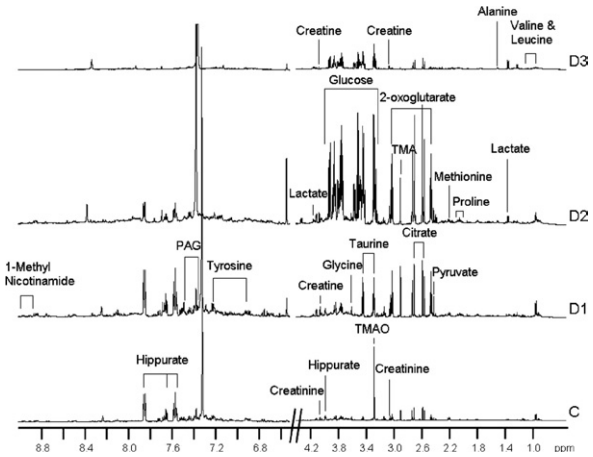

Figure 1. Representative 1-dimensional ^{1}H NMR spectra of control (C) and after administration of cisplatin 24 hours postdosing (D1), 48 hours postdosing (D2), and 72 hours postdosing (D3).

hours postdosing. Principal component analysis (PCA) of the spectral integrals showed distinct clusters for control urine and for urine collected on days 1, 2, and 3 after cisplatin injection, as shown in Figure 2. The loadings plot (data not shown) indicated that increases in proton resonances associated with 2-oxoglutarate and creatinine were the major metabolites separating day 1 samples from control, whereas increases in the glucose and lactate chemical shifts drove the clustering of the day 2 and day 3 urine samples away from control samples. Analysis of the spectra showed that the concentration of 2-oxoglutarate increased over the first 48 hours after dosing followed by a decrease from 48 to 72 hours. Figure 3 shows the 3-dimensional PCA plot obtained from analysis of day 2 urine samples from 4 groups of 4 mice each. These groups included control mice shown in solid circles, mice administered a single dose of cisplatin shown in solid squares, and 2 groups, one maintained on a special diet of WY-14,643 alone, and the other one maintained on the fibrate diet for 7 days before cisplatin injection shown in open triangles and plus signs, respectively. The PCA plot shows that the 4 groups separate into distinct clusters, with the control group on the special diet clustered fairly close to the control group on a normal diet. The cisplatin group clustered below the 3 groups along the PC3 axis.

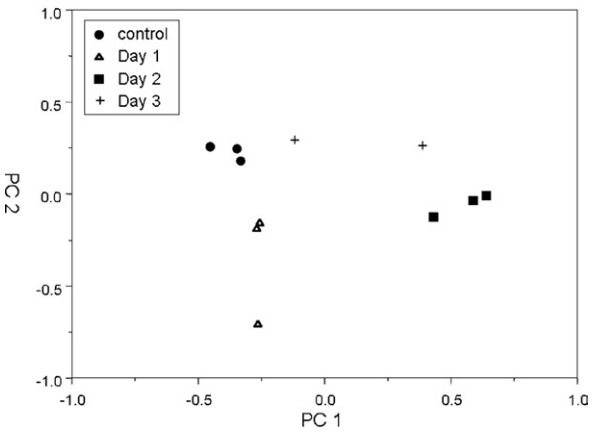

Figure 2. Principal component (PC) score plot showing the changes from control over a 72-hour period after administration of cisplatin. (●) Control animals, (Δ) 24 hours after dosing, (■) 48 hours after dosing, and (+) 72 hours after dosing.

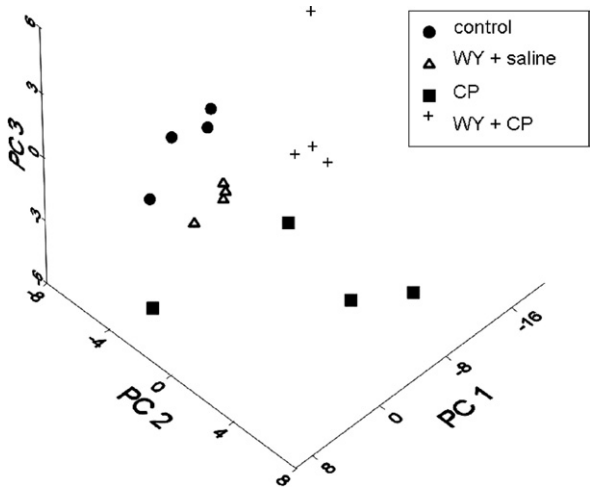

Figure 3. Three-dimensional PCA score plot of NMR data of day 2 urine indicating the effects of the PPARα ligand (WS) on cisplatin-induced ARF. (●) Control animals, (■) animals fed WY, (Δ) animals administered cisplatin after feeding with WY, and (+) animals administered cisplatin.

Quantitative analysis of select metabolites is shown in Table 1 and indicated that cisplatin treatment for 2 days induced significant changes in the urine levels of glucose (200-fold increase), alanine (12-fold increase), lactate (4-fold increase), leucine (7-fold increase), methionine (4-fold increase), 2-oxoglutarate (2-fold increase), pyruvate (3.5-fold increase), and valine (8-fold increase). Pretreatment with the diet containing PPARα ligand WY provided protection from the metabolic changes induced by

Table 1. Select Urine Metabolite Concentrations Measured by ^{1}H NMR Spectroscopy and Normalized to the Concentration of Creatinine in the Urine

Metabolite	Control (N = 7)	Cisplatin Day 2 (N = 7)	WY (N = 7)	WY + Cisplatin Day 2 (N = 7)
Alanine	0.02 ± 0.02	0.25 ± 0.13* $P = .003$	0.07 ± 0.06	0.19 ± 0.16* $P = .037$
Glucose	0.30 ± 0.30	60.98 ± 34.82* $P = .004$	0.66 ± 0.61	18.08 ± 23.98
Lactate	0.21 ± 0.30	0.89 ± 0.95	0.43 ± 0.37	0.57 ± 0.31
Leucine	0.03 ± 0.02	0.22 ± 0.10* $P = .004$	0.04 ± 0.01	0.28 ± 0.36
Methionine	0.03 ± 0.01	0.13 ± 0.07* $P = .009$	0.02 ± 0.01	0.05 ± 0.07
1-Methylnicotinamide	0.11 ± 0.06	0.07 ± 0.02	0.24 ± 0.12* $P = .038$	0.22 ± 0.08* $P = .016$
2-Oxoglutarate	7.97 ± 5.37	15.79 ± 2.78* $P = .008$	15.60 ± 3.76* $P = .010$	6.77 ± 3.21
Proline	0.26 ± 0.18	0.41 ± 0.22	0.46 ± 0.42	0.50 ± 0.41
Pyruvate	0.12 ± 0.07	0.44 ± 0.21* $P = .008$	0.22 ± 0.08* $P = .043$	0.27 ± 0.18
Trimethylamine	0.90 ± 0.89	0.28 ± 0.26	0.07 ± 0.06* $P = .048$	0.10 ± 0.09
Tyrosine	0.17 ± 0.08	0.15 ± 0.06	0.50 ± 0.56	0.41 ± 0.39
Valine	0.02 ± 0.01	0.16 ± 0.09* $P = .006$	0.02 ± 0.01	0.25 ± 0.36

NOTE. Values are reported as mg metabolite/mg creatinine.

cisplatin by reducing urine levels of glucose, lactate, methionine, 2-oxoglutarate, and pyruvate. The data also indicate that the PPARα ligand increased in urine levels of amino acids proline and tyrosine when compared with control or saline-treated mice. In addition, metabolite analysis showed that 1-methylnicotinamide was increased in both groups maintained on the diet containing PPARα ligand WY-16,463. This metabolite has been shown recently to be a biomarker for peroxisome proliferation.[23]

Cisplatin Increases Nonesterified Fatty Acids in Serum, Urine, and Kidney Tissue

Because neutral lipid accumulation detected by oil-red-O stain (Sigma, St. Louis, MO) represents the accumulation of nonesterified fatty acids (NEFAs), triglycerides, diglycerides, and cholesterol esters, we next examined specifically the effects of cisplatin on NEFA levels measured in serum, urine, and kidney tissue. As shown in Figure 4A, cisplatin-treated mice showed a time-dependent increase in NEFA levels not only in serum and urine, but also in kidney tissue. At day 3 there was a 3-fold increase in serum levels, and also at day 3 after cisplatin injection there was a 7-fold increase in kidney tissue levels of NEFAs. Our assay did not detect NEFA in the urine samples obtained from saline-treated mice. However, in cisplatin-treated mice there was a detectable level of NEFA in the urine obtained at day 3 after cisplatin injection (0.15 ± 0.01 mEq/L/mg protein).

PPARα Ligand Prevents Cisplatin-Induced Accumulation of NEFAs

Our most recent studies have shown that the use of PPARα ligands prevents the development of cisplatin-induced proximal tubule cell death by preventing the inhibition of fatty acid oxida-

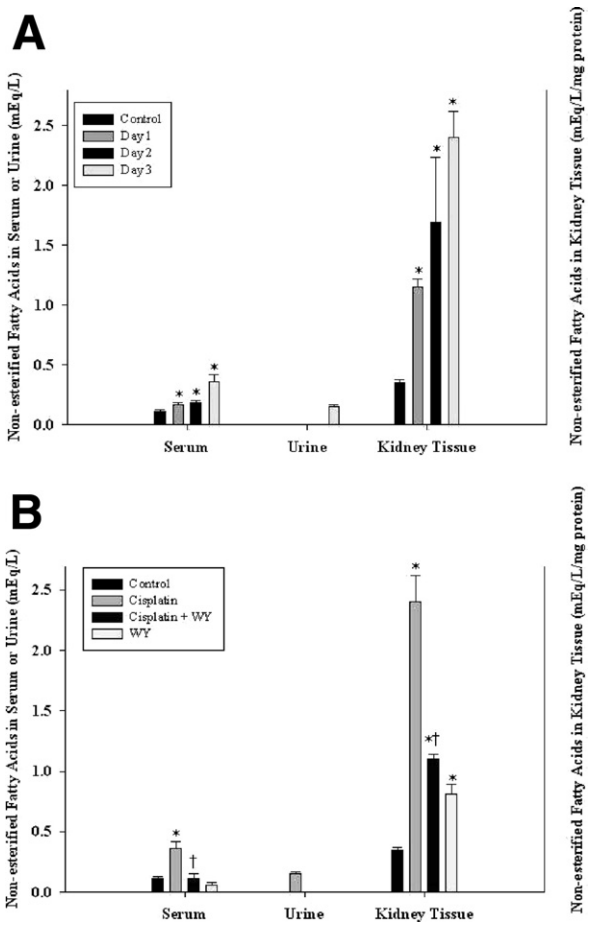

Figure 4. (A) Effect of cisplatin on NEFA levels in serum, urine, and kidney tissue. Mice were administered saline (control) or cisplatin (20 mg/kg/body weight) by a single intraperitoneal injection. NEFA levels were measured at day 1, day 2, and day 3 after cisplatin injection in serum, urine, and kidney tissue homogenates. Bars correspond to means ± SE of at least 6 independent experiments under each condition. *$P < .05$, compared with control by unpaired Student *t* test. (B) Effect of cisplatin and fibrate (WY) on NEFA levels. Wild-type mice were fed with either a regular or WY-containing diet and then were given saline (control and WY groups) or cisplatin (cisplatin and cisplatin + WY groups). NEFA levels were measured at day 3 after cisplatin injection in serum, urine, and kidney tissue homogenates as described in the Methods section. Results are expressed as the means ± SE. †$P < .05$ compared with cisplatin, *$P < .05$, compared with control by unpaired Student *t* test.

tion.[24] Therefore, we examined the effect of PPARα ligand on cisplatin-induced increased NEFA levels in serum, urine, and kidney tissue. At day 3 after cisplatin injection, there was a 3-fold increase in the serum levels of NEFA. In contrast, the group of mice that received the diet containing PPARα ligand and cisplatin showed comparable levels of serum NEFA with the mice treated with saline alone, as shown in Figure 4B. We also measured NEFA levels in urine samples of mice treated with PPARα ligand and cisplatin, and again similarly to saline-treated mice, we were not able to detect measurable amounts of NEFAs in the urine samples from these mice. We next examined the effect of PPARα ligand on cisplatin-mediated accumulation of NEFAs in kidney tissue. In the group of mice that received the diet containing PPARα ligand and cisplatin, there was a 65% reduction in the levels of NEFA in kidney tissue when compared with cisplatin-treated mice. These results are shown in Figure 4B.

Cisplatin Increases Triglyceride Levels in Serum and Kidney Tissue

Because triglycerides (TGs) represent the major component of neutral lipids in kidney tissue, we measured TG levels in serum, urine, and kidney tissue homogenates of mice treated with saline (control) and mice treated with cisplatin. As shown in Figure 5A we were able to detect TGs only in the serum and kidney tissue homogenates. Our assay was not able to detect measurable amounts of TGs in urine samples obtained from control or cisplatin-treated mice. As shown in Figure 5A, cisplatin-treated mice showed not only a time-dependent increase in TG levels in serum, but also in kidney tissue. At day 3 there was a 3-fold increased in serum TG levels, and also at day 3 after cisplatin injection there was a 6-fold increase in TG levels in kidney tissue homogenates.

PPARα Ligand Prevents Cisplatin-Induced Accumulation of TGs

We next examined the effect of PPARα ligand on cisplatin-mediated increased levels of TG in serum and kidney tissue. At day 3 after cisplatin injection, there was a 3-fold increase in the serum levels of TGs. In contrast, the group of mice that received the diet containing PPARα ligand and cisplatin showed a 70% reduction in serum TG levels when compared with cisplatin-treated mice, as shown in Figure 5B. We also examined the effect of PPARα ligand on cis-

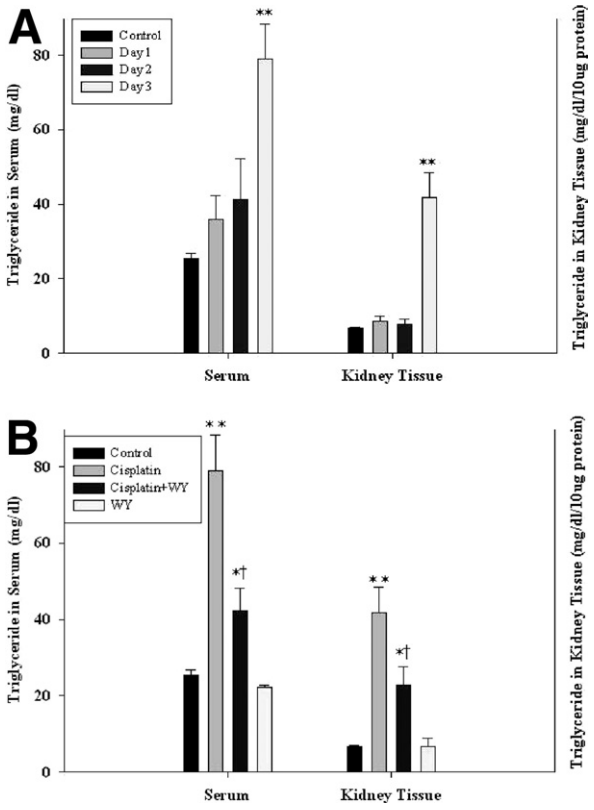

Figure 5. (A) Effect of cisplatin on TG levels in serum, urine, and kidney tissue. Mice were administered saline (control) or cisplatin (20 mg/kg/body weight) by a single intraperitoneal injection. TG levels were measured in serum, urine, and kidney tissues at day 1, day 2, and day 3 after cisplatin injection. Bars correspond to means ± SE of at least 6 independent experiments under each condition. $^{**}P < .005$ compared with control by unpaired Student *t* test. (B) Effect of cisplatin and fibrate (WY) on TG levels. Wild-type mice were fed with either a regular diet or WY-containing diet and then were given saline (control and WY groups) or cisplatin (cisplatin and cisplatin + WY groups). TG levels were measured in serum and kidney tissue homogenates at day 3 after cisplatin injection as described in the Methods section. Results are expressed as the means ± SE. $\dagger P < .05$ compared with cisplatin, $^{*}P < .05$, $^{**}P < .005$ compared with control by unpaired Student *t* test.

platin-mediated accumulation of TGs in kidney tissue. In the group of mice that received the diet containing PPARα ligand and cisplatin there was a 55% reduction in TG levels in kidney tissue when compared with cisplatin-treated mice. These results are shown in Figure 5B.

Cisplatin-Induced Hyperglycemia and Glucosuria Precede Cisplatin-Induced ARF

^{1}H NMR analysis of urine samples revealed that glucose was present within the first 24 to 48 hours postdosing with cisplatin. To corroborate these findings, we measured glucose levels in serum, urine, and kidney tissue by an enzymatic

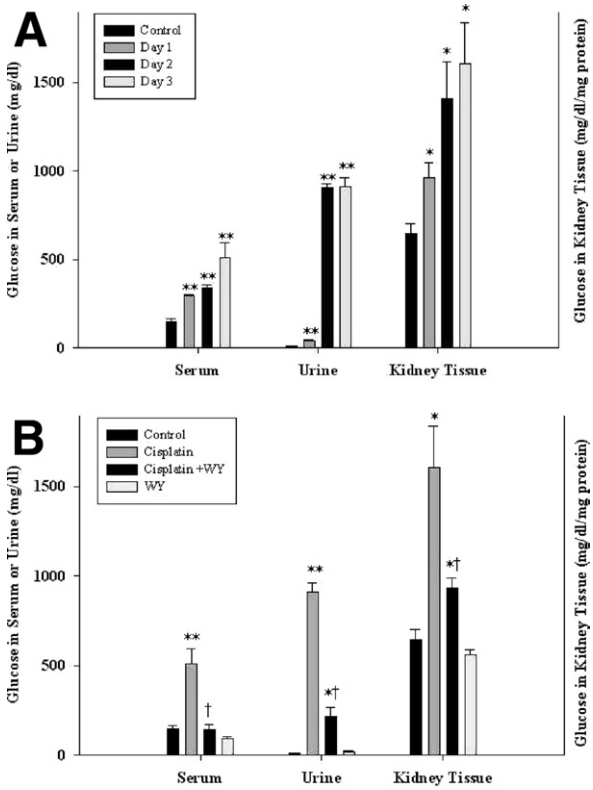

Figure 6. (A) Effect of cisplatin on glucose levels in serum, urine, and kidney tissue. Mice were administered saline (control) or cisplatin (20 mg/kg/body weight) by a single intraperitoneal injection. Glucose levels were measured at day 1, day 2, and day 3 after cisplatin injection in serum, urine, and kidney tissue homogenates. Bars correspond to means ± SE of at least 6 independent experiments under each condition. $^{*}P < .05$, $^{**}P < .005$ compared with control by unpaired Student *t* test. (B) Effect of cisplatin and fibrate (WY) on glucose levels. Wild-type mice were fed with either a regular or WY-containing diet and then were given saline (control and WY groups) or cisplatin (cisplatin and cisplatin + WY groups). Glucose levels were measured at day 3 after cisplatin injection in serum, urine, and kidney tissue homogenates as described in the Methods section. Results are expressed as the means ± SE. $\dagger P < .05$ compared with cisplatin, $^{*}P < .05$, $^{**}P < .005$ compared with control by unpaired Student *t* test.

colorimetric assay. As shown in Figure 6A, cisplatin induced a time-dependent increase in glucose levels in serum, urine, and kidney tissue. At day 3 after cisplatin injection there was a 3.5-fold increase in serum glucose levels when compared wit saline-treated mice. Cisplatin-treated mice also showed a remarkable 75-fold increase in urine glucose levels, and a 2.5-fold increase in kidney tissue levels of glucose, when compared with saline-treated mice.

PPARα Ligand Prevents Cisplatin-Induced Hyperglycemia and Glucosuria

Our most recent studies have shown that the use of PPARα ligands prevent the development of proximal tubule cell death during ARF by preventing not only fatty acid oxidation, but also by preventing the inhibition of pyruvate dehydrogenase complex (PDC) activity in the mitochondria.[24] In addition to its stimulation of fatty acid oxidation and anti-apoptotic effects, recent reports have suggested that PPARα also may play a role in the regulation of metabolic abnormalities associated with the metabolic syndrome.[25] Therefore, we examined the effect of PPARα ligand on cisplatin-induced increased levels of glucose in serum, urine, and kidney tissue. As shown in Figure 6B, serum glucose levels of wild-type mice receiving a regular diet were increased significantly by cisplatin treatment. At day 3, there was a 3.5-fold increase in serum glucose levels. By contrast, cisplatin-treated mice receiving a PPARα ligand in their diet showed comparable levels of serum glucose with the mice treated with saline alone. Similar to our NMR results, our biochemical analysis confirmed that cisplatin-treated mice showed remarkable increases in urine glucose levels (75-fold) when compared with saline-treated mice. In the group of mice that received the diet containing PPARα ligand and cisplatin, there was a 78% reduction in urine glucose levels when compared with cisplatin-treated mice. We next examined the effect of PPARα ligand on cisplatin-mediated accumulation of glucose in kidney tissue. In the group of mice that received the diet containing PPARα ligand and cisplatin, there was a 70% reduction in glucose levels in kidney tissue homogenates when compared with cisplatin-treated mice. These results are shown in Figure 6B.

Effect of Cisplatin and Fibrate (WY) on Serum Levels of Insulin

In the next series of experiments, we measured the effects of cisplatin on serum insulin levels. Three days after one single injection of cisplatin there were significant increases in serum insulin levels from control to cisplatin-treated mice of 0.506 ± 0.11 to 0.926 ± 0.14 μg/L (N = 6, $P < .05$). By contrast, cisplatin-treated mice receiving the diet containing PPARα ligand showed comparable levels of insulin with the mice treated with saline alone, as shown in Table 2.

In summary, we found that cisplatin-induced ARF produces an endogenous metabolic profile revealed by ^{1}H NMR analysis of urine. As indicated in Table 1, the most marked changes induced by cisplatin, and revealed by NMR spectroscopy, occurred within the first 48 hours, and were characterized by increased concentrations of glucose, lactate, amino acids such as alanine, valine, leucine, methionine, and the presence of tricarboxylic acid (TCA) cycle me-

Table 2. Effect of Cisplatin and Fibrate (WY) on Serum Levels of Glucose, Insulin, NEFAs, and TGs

Serum	Control	3-Day Cisplatin	WY	WY + Cisplatin
Glucose, mg/dL	145.87 ± 17.00	507.33 ± 85.54*	91.2 ± 12.3	142.75 ± 26.78†
Insulin, ug/L	0.51 ± 0.11	0.93 ± 0.14	0.37 ± 0.28	0.33 ± 0.11
NEFA, mEq/L	0.11 ± 0.02	0.36 ± 0.05‡	0.06 ± 0.02	0.11 ± 0.04†
TG, mg/dL	25.33 ± 1.45	79.00 ± 9.46*	22.33 ± 0.33	42.33 ± 5.81†,‡

Results are expressed as the means ± SE.
*$P < .005$ compared with control by unpaired Student t test.
†$P < .05$ compared with cisplatin.
‡$P < .05$ compared with control by unpaired Student t test.

tabolites such as pyruvate and lactate in urine. Our results confirm previous studies in which quantitative changes by NMR spectroscopic metabolite patterns provided information on the location and severity of toxic lesions. Those studies detected the presence of glucosuria and aminoaciduria after exposure to known proximal tubule nephrotoxins such as gentamicin, mercuric chloride, and D-serine.[6,7,26] Glucosuria and enhanced excretion of amino acids are both strong indicators of proximal tubule damage in general, likely caused by impaired tubular reabsorption in the proximal tubule via sodium-dependent glucose transport. In the case of gentamicin, recent in vivo and in vitro studies performed in LLCPK1 cells, as well as in mouse kidney tissue, have shown that aminoglycoside antibiotics reduce glucose reabsorption in kidney tissue by reducing messenger RNA (mRNA), protein expression, and function of the sodium-dependent glucose transporter, which is located in the apical membrane of the proximal tubule.[27] Our most recent unpublished studies, using alpha-D-^{14}C-glucopyranoside to examine the effects of cisplatin on glucose uptake in LLCPK1 cells, also lends support to the hypothesis that the inhibition of sodium-dependent glucose transport represents an early intracellular event that precedes proximal tubule cell death when LLCPK1 cells are exposed to cisplatin. Therefore, it is quite possible that a common mechanism of proximal tubule nephrotoxicity for both gentamicin and cisplatin relates to reduced expression and function of sodium-dependent glucose transporters. This mechanism of proximal tubule nephrotoxicity explains our findings by NMR analysis of the early presence of glucosuria and aminoaciduria in cisplatin-treated mice.

PPARα Ligand Prevents Cisplatin-Induced Hyperglycemia and Glucose Accumulation in Kidney Tissue

Previous studies performed in rats have shown that cisplatin-induced hyperglycemia is secondary to the presence of marked glucose intolerance, in association with an impaired insulin response and an abnormal glucagon response to a glucose stimulus.[28,29] Our studies corroborate those previous findings in mice treated with cisplatin, including the presence of severe hyperglycemia, as well as the presence of hyperinsulinemia, as shown in Table 2. In addition, our studies also confirmed the presence of an inappropriate insulin response when compared with the level of hyperglycemia induced by cisplatin in these mice. On the other hand, fibrate treatment significantly ameliorated cisplatin-induced hyperglycemia and hyperinsulinemia, and also prevented cisplatin-mediated accumulation of glucose in kidney tissue. These results suggest that fibrate treatment leads to an improved insulin action in kidney tissue. This beneficial effect of fibrates or PPARα ligands on hyperglycemia and insulin levels has been observed previously in animal models of diabetes, and also in diabetes-prone animals.[30-32] By using Otsuka Long Evans Tokushima Fatty rats, Koh et al[33] showed that fibrate treatment prevented the development of diabetes by several mechanisms that included: (1) reduced basal plasma insulin concentrations, (2) reduced adiposity, (3) improved peripheral insulin action, and (4) by exerting beneficial effects on pancreatic β-cell function.

Cisplatin-Mediated Renal Lipid Accumulation Is Ameliorated by PPARα Ligand

A previous study had reported that cisplatin nephrotoxicity in rats was accompanied by significant increases in serum total cholesterol and TG concentrations, an effect that was not accompanied by injury to the liver.[34] Our results extend those previous observations, showing also accumulation of TGs and NEFAs in kidney tissue of cisplatin-treated mice. The mechanisms by which cisplatin increases both NEFA and TG accumulation in kidney tissue likely reflect in part cisplatin-mediated inhibition of fatty acid oxidation. We have shown that cisplatin causes a significant reduction in mRNA levels and enzyme activity of mitochondrial medium chain acyl-CoA dehydrogenase (MCAD), and that the use of PPARα ligand WY prevented cisplatin-induced reduction of mRNA levels and enzyme activity of MCAD and ameliorated ARF.[24] By contrast, cisplatin-treated PPARα null mice fail to show a protective effect of fibrate treatment and do not reverse

cisplatin-mediated inhibition of MCAD.[24] In our most recent study, performed in renal epithelial cells in culture, we found that cisplatin directly inhibited PPARα activity in these cells, and this event was accompanied by increased accumulation of NEFAs.[35] Pretreatment with fibrate prevented the inhibition of PPARα activity, and the accumulation of NEFAs, and also prevented cisplatin-induced proximal tubule cell death, supporting our in vivo observations about the protective role of PPARα ligands in reducing accumulation of NEFAs and preventing cisplatin-mediated nephrotoxicity.

In addition to the protective effects of fibrates in preventing cisplatin-mediated inhibition of fatty acid oxidation in kidney tissue, our study cannot rule out the presence of protective systemic effects of fibrates on kidney tissue lipotoxicity. For example, the most pronounced systemic effect of fibrates is to reduce plasma TG-rich lipoproteins. The hypotriglyceridemic action of fibrates involves combined effects on lipoprotein lipase (LPL) and apo-CIII expression,[33] resulting in increased lipolysis. The induction of LPL expression occurs at the transcriptional level and is mediated by PPARα. In contrast to LPL, transcription of the apoCIII gene is inhibited by fibrates, resulting in decreased production of apoCIII in the liver and reduced serum TG levels.[36] The repression of apoCIII gene expression by fibrates is mediated by PPARα.[37] Previous studies also have shown that in addition to increased lipolysis, fibrates also increase the hepatic uptake of free fatty acids by inducing the expression of specific fatty acid transport proteins and by increasing the formation of acyl CoA esters by acyl CoA synthetase.[38] Therefore, fibrates potentially could change free fatty acid metabolism from TG synthesis to catabolism. Additional cellular mechanisms by which cisplatin increases the accumulation of TG in the proximal tubule are likely to be involved. In a recent study by Peters et al,[39] the investigators examined the potential mechanisms by which proximal tubule injury leads to TG accumulation. Significant differences in the expression and function of TG synthetic and degradative pathways were found, depending on the in vivo or in vitro model of tubular cell damage used. A significantly increased expression in acyl coenzyme A:diacylglycerol acyltransferase expression was seen in the antimycin and endotoxin models, whereas reduced expression of TG lipase was seen in the glycerol model of ARF. Although we have not examined in detail the cellular mechanisms by which cisplatin induces TG accumulation in the proximal tubule, our recent gene-array analysis of kidney tissue of mice treated with cisplatin showed that mRNA levels of fatty acid synthetase gene were reduced significantly by cisplatin. This observation suggests that reduced TG catabolism by cisplatin and increased accumulation of free fatty acids represent important mechanism(s) of TG accumulation in the proximal tubule.

In summary, our analysis by NMR spectroscopy shows that exposure to cisplatin results in a marked change in the urinary metabolic profile that precedes changes in known biomarkers of nephrotoxicity, such as blood urea nitrogen and serum creatinine. Future analysis by ultra performance liquid chromatography (UPLC)/MS-based techniques should allow us to further differentiate the presence of spurious markers that merely reflect the administration of cisplatin from genuine biomarkers of toxicity. In addition, our results further support the protective role of PPARα ligands on renal function by preventing systemic and renal alterations in glucose and lipid metabolism caused by cisplatin.

SYSTEMS TOXICOLOGY: INTEGRATED METABONOMICS AND PROTEOMICS IN LIVER TISSUE

Although our studies focused solely on metabolomic analysis, others have sought to integrate metabolomic and proteomic analyses. Metabonomics, proteomics, and gene expression microarray platforms were used in a systems biology study of acute hepatotoxicity of valproic acid.[40] Pregnant CD-1 mice were injected subcutaneously with 600 mg/kg valproic acid or vehicle control. Urine, serum, and liver tissue were collected at 6, 12, and 24 hours after dosing. One-dimensional proton NMR experiments were applied to the urine and aqueous extracts of terminal plasma and tissue samples using a Bruker 600 MHz NMR. PCA of the binned NMR spectral data of urine samples

showed the valproic acid (VPA)-dosed groups were clustered away from the controls as a result of altered glucose concentrations in urine samples at 12 and 24 hours. NMR metabonomics procedures applied on aqueous liver tissue extracts showed altered glucose levels at 12 hours after VPA administration. Proteomics was applied to crude liver mitochondrial-enriched fractions that were prepared from 24-hour control and VPA-treated mouse liver homogenates. Approximately 30 μg from each pooled sample was dissolved in loading buffer and separated by sodium dodecyl sulfate–polyacrylamide gel electrophoresis. The sodium dodecyl sulfate gel was sliced into 38 bands and were transferred to a 96-well plate. Gel bands were reduced with dithiothreitol, alkylated with iodoacetamide, and digested with trypsin as previously described.[41,42] The resultant 50-μL peptide pools were analyzed using nano LC/mass spectrometry (MS)/MS on a LCQ Deca XP Plus ion trap mass spectrometer (Waltham, MA). Samples were eluted with a 50-minute gradient and MS/MS was performed on the top 4 ions in each MS scan using the data-dependent acquisition mode. Product ion data were searched against the European Bioinformatics Institute's mouse international protein index protein database. Proteomics studies identified 2 proteins, glycogen phosphorylase and amylo-1,6-glucosidase, which were increased in dosed animals relative to control. Both of these proteins are involved in converting glycogen to glucose. The combined metabolomic and proteomic studies indicated a perturbation in the glycogenolysis pathway after administration of valproic acid.

CONCLUSIONS

The application of metabolomics to evaluate and monitor the presence of acute kidney disease is still under development. From the work presented in this review, it is apparent that a number of known and unknown metabolites that can be measured easily in urine, serum, and kidney tissue could provide a reliable indication of organ function. Validation of these metabolic biomarkers with respect to preclinical and clinical use, sensitivity, and specificity could provide additional tools in the detection of the onset and severity of kidney injury. Moreover, a significant opportunity exists to integrate metabolomic and proteomic analyses in the study of renal pathophysiology. The literature indicates that the 2 approaches have yet to be applied in a single study of renal function or pathology. The application of such a systems biology approach is likely to provide new insights into renal disease.

REFERENCES

1. Vaidya VS, Bonventre JV. Mechanistic biomarkers for cytotoxic acute kidney injury. Expert Opin Drug Metab Toxicol. 2006;2:697-713.
2. Fiehn O. Metabolomics—the link between genotypes and phenotypes. Plant Mol Biol. 2002;48:155-71.
3. Nicholson JK, Lindon JC, Holmes E. 'Metabonomics': understanding the metabolic responses of living systems to pathophysiological stimuli via multivariate statistical analysis of biological NMR spectroscopic data. Xenobiotica. 1999;29:1181-9.
4. Raamsdonk LM, Teusink B, Broadhurst D, Zhang N, Hayes A, Walsh MC, et al. A functional genomics strategy that uses metabolome data to reveal the phenotype of silent mutations. Nat Biotechnol. 2001;19:45-50.
5. Robertson DG, Reily MD, Sigler RE, Wells DF, Paterson DA, Braden TK. Metabonomics: evaluation of nuclear magnetic resonance (NMR) and pattern recognition technology for rapid in vivo screening of liver and kidney toxicants. Toxicol Sci. 2000;57:326-37.
6. Williams RE, Jacobsen M, Lock EA. 1H NMR pattern recognition and 31P NMR studies with D-serine in rat urine and kidney, time- and dose-related metabolic effects. Chem Res Toxicol. 2003;16:1207-16.
7. Lenz EM, Bright J, Knight R, Westwood FR, Davies D, Major H, et al. Metabonomics with 1H-NMR spectroscopy and liquid chromatography-mass spectrometry applied to the investigation of metabolic changes caused by gentamicin-induced nephrotoxicity in the rat. Biomarkers. 2005;10:173-87.
8. Serkova N, Fuller TF, Klawitter J, Freise CE, Niemann CU. H-NMR based metabolic signatures of mild and severe ischemia/reperfusion injury in rat kidney transplants. Kidney Int. 2005;67:1142-51.
9. Portilla D, Li S, Nagothu K, Megyesi J, Schnackenberg L, Safirstein RL, et al. Metabolomic study of cisplatin-induced nephrotoxicity. Kidney Int. 2006;69:2194-204.
10. Schnackenberg LK, Dragan YP, Reily MD, Robertson DG, Beger RD. Evaluation of NMR spectral data of urine in conjunction with measured clinical chemistry and histopathology parameters to assess the effects of liver and kidney toxicants. Metabolomics. 2007;3:87-100.
11. Coen M, Lenz EM, Nicholson JK, Wilson ID, Pognan F, Lindon JC. An integrated metabonomic investigation

of acetaminophen toxicity in the mouse using NMR spectroscopy. Chem Res Toxicol. 2003;16:295-303.
12. Schnackenberg L, Beger RD, Dragan Y. NMR-based metabonomic evaluation of livers from rats chronically treated with tamoxifen, mestranol, and phenobarbital. Metabonomics. 2005;1:87-94.
13. Waters NJ, Waterfield CJ, Farrant RD, Holmes E, Nicholson JK. Integrated metabonomic analysis of bromobenzene-induced hepatotoxicity: novel induction of 5-oxoprolinosis. J Proteome Res. 2006;5:1448-59.
14. Serkova N, Fuller TF, Klawitter J, Freise CE, Niemann CU. H-NMR-based metabolic signatures of mild and severe ischemia/reperfusion injury in rat kidney transplants. Kidney Int. 2005;67:1142-51.
15. Odunsi K, Wollman RM, Ambrosone CB, Hutson A, McCann SE, Tammela J, et al. Detection of epithelial ovarian cancer using 1H-NMR-based metabonomics. Int J Cancer. 2005;113:782-8.
16. Beger RD, Schnackenberg LK, Li D, Dragan Y. Metabonomic models of human pancreatic cancer using 1D proton NMR spectra of lipids in plasma. Metabolomics. 2006;2:125-34.
17. Brindle JT, Antti H, Holmes E, Tranter G, Nicholson JK, Bethel HWL, et al. Rapid and noninvasive diagnosis of the presence and severity of coronary heart disease using 1H-NMR-based metabonomics. Nat Med. 2002;8:1439-45.
18. Mayr M, Chung YL, Mayr U, Yin X, Ly L, Troy H, et al. Proteomic and metabolomic analyses of atherosclerotic vessels from apolipoprotein E-deficient mice reveal alterations in inflammation, oxidative stress, and energy metabolism. Arterioscler Thromb Vasc Biol. 2005;25:2135-42.
19. Naziroglu M, Karaoglu A, Aksoy AO. Selenium and high dose vitamin E administration protects cisplatin-induced oxidative damage to renal, liver and lens tissues in rats. Toxicology. 2004;195:221-30.
20. Price PM, Safirstein RL, Megyesi J. Protection of renal cells from cisplatin toxicity by cell cycle inhibitors. Am J Physiol. 2004;286:F378-84.
21. Atasoyu EM, Yildiz S, Bilgi O, Cermik H, Evrenkaya R, Aktas S, et al. Investigation of the role of hyperbaric oxygen therapy in cisplatin-induced nephrotoxicity in rats. Arch Toxicol. 2005;79:289-93.
22. Santos NA, Catao CS, Martins NM, Curti C, Bianchi ML, Santos AC.Cisplatin-induced nephrotoxicity is associated with oxidative stress, redox state unbalance, impairment of energetic metabolism and apoptosis in rat kidney mitochondria. Arch Toxicol. 2007;81:495-504.
23. Delaney J, Hodson MP, Thakkar H, Connor SC, Sweatman BC, Kenny SP, et al. Tryptophan-NAD+ pathway metabolites as putative biomarkers and predictors of peroxisome proliferation. Arch Toxicol. 2005;79:208-23.
24. Li S, Wu P, Yarlagadda P, Vadjunec NM, Proia AD, Harris RA, et al. PPAR alpha ligand protects during cisplatin-induced acute renal failure by preventing inhibition of renal FAO and PDC activity. Am J Physiol. 2004;286:F572-80.
25. Chinetti-Gbaguidi G, Fruchart JC, Staels B. Role of the PPAR family of nuclear receptors in the regulation of metabolic and cardiovascular homeostasis: new approaches to therapy. Curr Opin Pharmacol. 2005;5: 177-83.
26. Lenz EM, Bright J, Knight R, Wilson ID, Major H. A metabonomic investigation of the biochemical effects of mercuric chloride in the rat using 1H NMR and HPLC-TOF/MS: time dependent changes in the urinary profile of endogenous metabolites as a result of nephrotoxicity. Analyst. 2004;129:535-41.
27. Fleck C, Schwertfeger M, Taylor PM. Regulation of renal amino acid (AA) transport by hormones, drugs and xenobiotics—a review. Amino Acids. 2003;24: 347-74.
28. Fleck C, Kretzschel I, Sperschneider T, Appenroth D. Renal amino acid transport in immature and adult rats during chromate and cisplatinum-induced nephrotoxicity. Amino Acids. 2001;20:201-15.
29. Takamoto K, Kawada M, Usui T, Ishizuka M, Ikeda D. Aminoglycoside antibiotics reduce glucose reabsorption in kidney through down-regulation of SGLT1. Biochem Biophys Res Commun. 2003;308:866-71.
30. Goldstein RS, Mayor GH, Rosenbaum RW, Hook JB, Santiago JV, Bond JT. Glucose intolerance following cis-platinum treatment in rats. Toxicology. 1982;24: 273-80.
31. Goldstein RS, Mayor GH, Gingerich RL, Hook JB, Rosenbaum RW, Bond JT. The effects of cisplatin and other divalent platinum compounds on glucose metabolism and pancreatic endocrine function. Toxicol Appl Pharmacol. 1983;69:432-41.
32. Jia D, Otsuki M. Bezafibrate, a peroxisome proliferator-activated receptor (PPAR)-alpha activator, prevents pancreatic degeneration in obese and diabetic rats. Pancreas. 2003;26:286-91.
33. Koh EH, Kim MS, Park JY, Kim HS, Youn JY, Park HS, et al. Peroxisome proliferator-activated receptor (PPAR)-alpha activation prevents diabetes in OLETF rats: comparison with PPAR-gamma activation. Diabetes. 2003;52:2331-7.
34. Bihan H, Rouault C, Reach G, Poitout V, Staels B, Guerre-Millo M. Pancreatic islet response to hyperglycemia is dependent on peroxisome proliferator-activated receptor alpha (PPARalpha). FEBS Lett. 2005; 579:2284-8.
35. Nagothu KK, Bhatt R, Kaushal GP, Portilla D. Fibrate prevents cisplatin-induced proximal tubule cell death. Kidney Int. 2005;68:2680-93.
36. Abdel-Gayoum AA, El-Jenjan KB, Ghwarsha KA. Hyperlipidaemia in cisplatin-induced nephrotic rats. Hum Exp Toxicol. 1999;18:454-9.
37. Staels B, Vu-Dac N, Kosykh VA, Saladin R, Fruchart JC, Dallongeville J, et al. Fibrates downregulate apolipoprotein C-III expression independent of induction of peroxisomal acyl coenzyme A oxidase. A potential

mechanism for the hypolipidemic action of fibrates. J Clin Invest. 1995;95:705-12.
38. van Dijk KW, Rensen PC, Voshol PJ, Havekes LM. The role and mode of action of apolipoproteins CIII and AV: synergistic actors in triglyceride metabolism? Curr Opin Lipidol. 2004;15:239-46.
39. Peters JM, Hennuyer N, Staels B, Fruchart JC, Fievet C, Gonzalez FJ, et al. Alterations in lipoprotein metabolism in peroxisome proliferator-activated receptor alpha-deficient mice. J Biol Chem. 1997;272:27307-12.
40. Schnackenberg LK, Jones RC, Thyparambil S, Taylor JT, Han T, Tong W, et al. An integrated study of acute effects of valproic acid in the liver using metabonomics, proteomics, and transcriptomics platforms. OMICS. 2006;10:1-14.
41. Edmonson RD, Vondriska TM, Biederman KJ, Zhang J, Jones RC, Zheng Y, et al. Protein kinase C epsilon signaling complexes include metabolism- and transcription/translation-related proteins: complimentary separation techniques with LC/MS/MS. Mol Cell Proteomics. 2002;1:421-33.
42. Gambus A, Jones RC, Sanchez-Diaz A, Kanemaki M, van Deursen F, Edmonson RD, et al. GINS-dependent replisome progression complex controls the advance of eukaryotic DNA replication forks. Nat Cell Biol. 2006;8:358-66.